Comprehensive analysis to identify DLEU2L/TAOK1 axis as a prognostic biomarker in hepatocellular carcinoma

Yi Shi,[1,2,3,11] Dan-Dan Zhang,[4,5,11] Ji-Bin Liu,[2,11] Xiao-Li Yang,[5,11] Rui Xin,[5,11] Cheng-You Jia,[6] Hui-Min Wang,[5] Gai-Xia Lu,[6] Pei-Yao Wang,[5] Yu Liu,[1,3] Zi-Jin Li,[1] Jing Deng,[1] Qin-Lu Lin,[1] Liang Ma,[3] Shan-Shan Feng,[3] Xiao-Qi Chen,[1] Xiang-Min Zheng,[3] Ya-Fu Zhou,[7] Yong-Jun Hu,[7] Hua-Qun Yin,[8] Lin-Lin Tian,[5] Li-Peng Gu,[5] Zhong-Wei Lv,[6] Fei Yu,[6] Wen Li,[1,3] Yu-Shui Ma,[6,9,10] and Fu Da[1,5]

[1]National Engineering Laboratory for Deep Process of Rice and Byproducts, College of Food Science and Engineering, Central South University of Forestry and Technology, Changsha 410004, Hunan, China; [2]Cancer Institute, Nantong Tumor Hospital, Nantong 226631, China; [3]College of Life Sciences and Chemistry, Hunan University of Technology, Zhuzhou 412007, Hunan, China; [4]Department of Pathology, Shihezi University School of Medicine, Shihezi 832002, Xinjiang, China; [5]Central Laboratory for Medical Research, Shanghai Tenth People's Hospital, Tongji University School of Medicine, Shanghai 200072, China; [6]Department of Nuclear Medicine, Shanghai Tenth People's Hospital, Tongji University School of Medicine, Shanghai 200072, China; [7]Department of Cardiology, Hunan Provincial People's Hospital, The First Affiliated Hospital of Hunan Normal University, Changsha 410005, Hunan, China; [8]School of Resource Processing and Bioengineering, Central South University, Changsha 410083, Hunan, China; [9]Department of Pancreatic and Hepatobiliary Surgery, Cancer Hospital, Fudan University Shanghai Cancer Center, Shanghai 200032, China; [10]Pancreatic Cancer Institute, Fudan University, Shanghai 200032, China

Hepatocellular carcinoma (HCC) is one of the deadliest malignant tumors that are harmful to human health. Increasing evidence has underscored the critical role of the competitive endogenous RNA (ceRNA) regulatory networks among various human cancers. However, the complexity and behavior characteristics of the ceRNA network in HCC were still unclear. In this study, we aimed to clarify a phosphatase and tensin homolog (PTEN)-related ceRNA regulatory network and identify potential prognostic markers associated with HCC. The expression profiles of three RNAs (long non-coding RNAs [lncRNAs], microRNAs [miRNAs], and mRNAs) were extracted from The Cancer Genome Atlas (TCGA) database. The DLEU2L-hsa-miR-100-5p/ hsa-miR-99a-5p-TAOK1 ceRNA network related to the prognosis of HCC was obtained by performing bioinformatics analysis. Importantly, we identified the DLEU2L/ TAOK1 axis in the ceRNA by using correlation analysis, and it appeared to become a clinical prognostic model by Cox regression analysis. Furthermore, methylation analyses suggested that the abnormal upregulation of the DLEU2L/ TAOK1 axis likely resulted from hypomethylation, and immune infiltration analysis showed that the DLEU2L/TAOK1 axis may have an impact on the changes in the tumor immune microenvironment and the development of HCC. In summary, the current study constructing a ceRNA-based DLEU2L/ TAOK1 axis might be a novel important prognostic factor associated with the diagnosis and prognosis of HCC.

INTRODUCTION

Liver cancer, mainly hepatocellular carcinoma (HCC), is the sixth most common cancer type and the fourth deadly cause of cancer in the world.[1] It has been estimated that, in 2018, there were 782,000 deaths and 841,000 new cases of liver cancer in the world, with a higher incidence in men than in women in many parts of the world.[2,3] Statistics indicate that the 5-year survival for HCC is 18%, which shows that only 30%–40% of patients were diagnosed in the early stage.[4] Curative-intent treatments for early stage HCC include surgical resection, ablation, liver transplantation (LT), and transarterial chemoembolization (TACE).[5] However, the main characteristics of HCC include a high rate of recurrence and metastasis, a low detection rate of curable stages, and ineffective treatments. Moreover, the incidence and mortality of HCC still continue to increase in many countries, and it has been generally recognized as a cancer with poor prognosis and reduced survival. Hence, it is essential to explore useful prognostic biomarkers and/or therapeutic targets for HCC to improve our deficiencies in the diagnosis, prevention, and treatment of the disease.

Correspondence: Wen Li, PhD, National Engineering Laboratory for Deep Process of Rice and Byproducts, College of Food Science and Engineering, Central South University of Forestry and Technology, 498 South Shaoshan Road, Changsha 410004, Hunan, China.
E-mail: liwen@hut.edu.cn
Correspondence: Yu-Shui Ma, PhD, Department of Nuclear Medicine, Shanghai Tenth People's Hospital, Tongji University School of Medicine, 36 Yunxin Road, Shanghai 200072, China.
E-mail: mayushui2006@126.com
Correspondence: Da Fu, PhD, Central Laboratory for Medical Research, Shanghai Tenth People's Hospital, Tongji University School of Medicine, 36 Yunxin Road, Shanghai 200072, China.
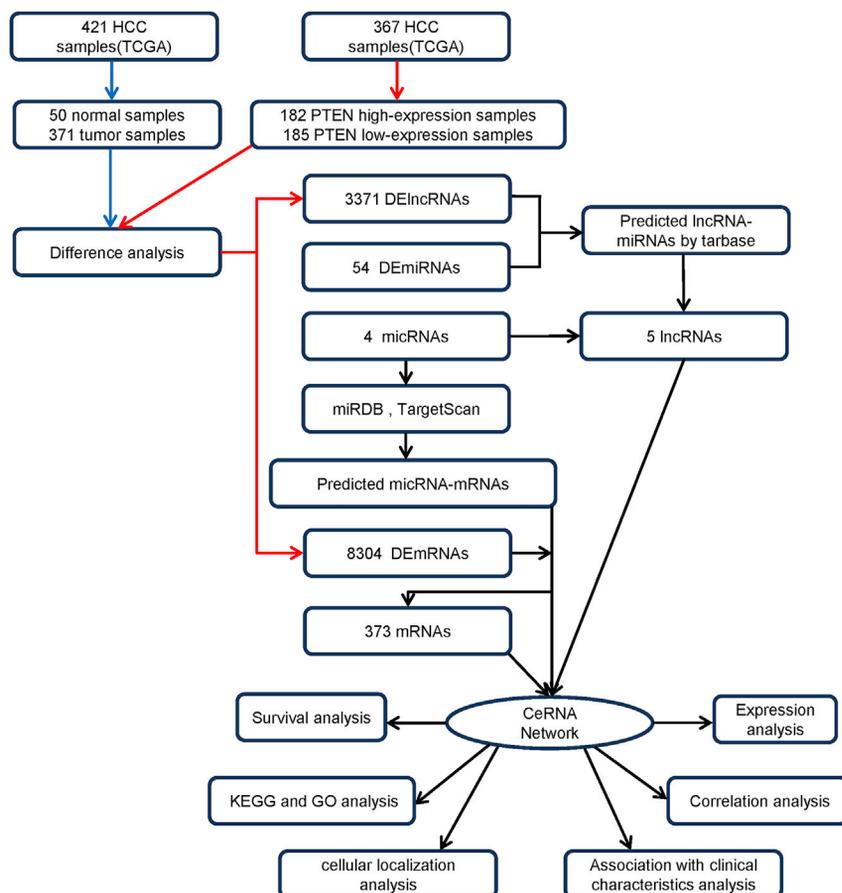**E-mail:** fu800da900@126.com

of its target mRNA to inhibit gene degradation or translation.[15–17] We have learned that miRNAs regulate approximately 30% of the genes in the human genome.[18] Moreover, miRNA-mediated post-transcriptional regulation requires multiple RNA-binding proteins, which are conducive to the function of miRNA in tumorigenesis.[19–21] In the cytoplasm, Salmena et al.[22] proposed the competitive endogenous RNA (ceRNA) hypothesis that lncRNA is described as mainly regulating mRNA through a ceRNA regulation mechanism. As far as HCC is concerned, for the selected example, Zhan et al.[23] demonstrated that HOXA11-AS, as an oncogene, can accelerate HCC growth through the miR-506-3p/Slug axis. Zhang et al.[24] identified that high levels of NEAT1 promoted the metastasis of HCC cells by acting as a miR-320a molecular sponge and targeting LAGE3. However, a study by Xu et al.[25] illustrated that overexpression of WWOX inhibited cell proliferation and metastasis by sponge miR-20b-5p.

Phosphatase and tensin homolog (PTEN) is a very commonly mutated tumor suppressor gene in human cancers, including HCC.[26–29] Accumulating evidence has shed light on PTEN activity, which can be regulated by mutations, epigenetic silencing, abnormal protein, transcriptional inhibition, localization, and posttranslational modification.[30–32] At the same time, some data have indicated that decreased PTEN expression is a common event in HCC and is associated with disease stage, tumor grade and size, and increased expression of tumor markers.[33–36]

It is well known that publicly available large-scale cancer omics data, such as The Cancer Genome Atlas (TCGA), provide us with clinical information and molecular data on various cancer patients, which may be very helpful for us to find candidate tumor biomarkers.[6] The widespread applications of high-throughput RNA sequencing (RNA-seq) resulted in the development of better noninvasive, repeatable, sensitive, and accurate tools used in early screening, diagnosis, evaluation, and monitoring of patients.

Long non-coding RNAs (lncRNAs) are broadly defined as a subtype of ncRNAs with a length greater than 200 nt that have no or limited protein-coding ability.[7] Several studies have shown that lncRNAs have direct and indirect regulatory effects in cancer biology.[8–10] It has been reported that these long molecules are frequently dysregulated in a variety of cancers, and in different types of cancers (including HCC), specific lncRNAs are associated with cancer recurrence, metastasis, and poor prognosis.[11–14] Therefore, it is thought that the specific lncRNA biomarkers related to the prognosis and diagnosis of HCC are of great clinical significance.

MicroRNAs (miRNAs), a kind of small single-stranded ncRNA, include 19–25 nt and can bind to the 3′ untranslated region (UTR)

In this study, we constructed a ceRNA network related to PTEN in HCC (Figure 1). First, through differential expression analysis in two groups of PTEN^{high} and PTEN^{low} expression in 371 HCC samples, the HCC-related lncRNA-miRNA-mRNA triple regulatory networks constructed from three differentially expressed RNAs were obtained. Functional enrichment analysis was conducted to assess the functional role and potential mechanism of the network in HCC. Then, a key ceRNA network was identified by expression analysis, survival analysis, and nuclear-cytoplasmic localization analysis of RNAs from hub triple regulatory networks. Moreover, we performed a correlation analysis between these four predictive genes and PTEN that showed that the DLEU2L/TAOK1 axis played a vital role in HCC. Finally, Cox regression analysis was carried out to obtain the diagnostic and prognostic values of TAOK1 in HCC, Gene Ontology (GO) and Kyoto Encyclopedia of Genes and Genomes (KEGG) analyses were utilized

to get the possible function of TAOK1 in HCC, and methylation analysis and immune infiltration analysis were further performed to study the potential biological function of TAOK1 in HCC.

RESULTS

The tumor suppressor role and prognostic value of PTEN overexpression in HCC

To investigate the possible role of PTEN in HCC, based on the Human Protein Atlas (HPA) database, we found that PTEN was overexpressed in normal hepatic tissue, but downexpressed in HCC tissues (Figures 2A and S1). Similar deregulation of PTEN expression was also demonstrated by immunohistochemistry (IHC) staining obtained from the HPA (Figure 2B), and the patient data from the IHC are listed in Table S1.

Since PTEN is abnormally downexpressed in tumor specimens, we then studied the clinical significance of PTEN expression in HCC patients. According to the Kaplan-Meier survival curves, as shown in Figure 2C, our data indicated that lower expression of PTEN markedly correlated with poor overall survival (OS) in patients of the HCC cohort.

Furthermore, to understand the potential mechanism of the abnormally low expression of PTEN in HCC, we analyzed the genomic and copy numbers of PTEN. The results of our analysis on cBioPortal are as follows, with an OncoPrint plot showing the deletion of PTEN gene in TCGA HCC dataset (Figure 2D).

As shown in Figure 1E, more than one-third of all HCC samples harbored PTEN deletion, and, consistently, HCC samples harboring PTEN deletion exhibited lower mRNA expression than did those that exhibit diploid PTEN. Additionally, a positive correlation between PTEN copy number value and mRNA expression was found in HCC samples (Figure 2F).

Taken together, these data demonstrate that PTEN expression is downregulated in HCC and that the deletion of PTEN copy numbers is likely to be one of the main mechanisms that make a contribution to the downregulation of PTEN among HCC patients.

Identification of differentially expressed genes (DEGs) (DEmRNAs, DElncRNAs, and DEmiRNAs)

According to the above analysis, the ceRNA network related to PTEN can be used as a potential prognostic model for HCC patients. Also, we must know that the meaning of the expression levels in HCC samples with PTEN^{high} and PTEN^{low} expression groups are opposite to those in cancer and paracancerous groups.

To verify this conjecture, we first identified the DElncRNAs, DEmiRNAs, and DEmRNAs in HCC samples with PTEN^{high} and PTEN^{low} expression groups as well as in HCC and adjacent normal tissues using TCGA database, with $p < 0.05$ and |log fold change [FC]| >0.5 as the lncRNA threshold, $p < 0.05$ and |logFC| >0.3 as the miRNA threshold, and $p < 0.05$ and |logFC| >0.7/0.5 as the mRNA threshold.

In total, 860 DElncRNAs (137 upregulated and 723 downregulated), 54 DEmiRNAs (21 upregulated and 33 downregulated), and 1,871 DEmRNAs (195 upregulated and 1676 downregulated) were sorted out from HCC samples with PTEN^{high} and PTEN^{low} expression groups.

Furthermore, a total of 3,371 DElncRNAs (3,041 upregulated and 330 downregulated), 420 DEmiRNAs (102 upregulated and 318 downregulated), and 8,294 DEmRNAs (7,059 upregulated and 1,235 downregulated) were identified between HCC samples and normal liver tissue samples. Volcano plots visually displaying the distribution of DElncRNAs, DEmiRNAs, and DEmRNAs were generated (Figures 3A–3C and S2A–S2C), and the heatmaps depict the expression of 15 significant variable genes in HCC samples with PTEN^{high} and PTEN^{low} expression, as well as in HCC and normal samples (Figures 3D–3F and S2D–S2F).

Construction of the lncRNA-miRNA-mRNA triple regulatory network

To establish the lncRNA-miRNA-mRNA triple regulatory network in HCC, we conducted a joint analysis in the PTEN^{high} and PTEN^{low} expression groups as well as in HCC and normal hepatic tissue groups. First, we put the remaining DElncRNAs into the TarBase database to identify potential miRNAs targeting lncRNAs. Four out of the predicted miRNAs were selected after taking the intersection with 54 DEmiRNAs. We then used the databases of miRDB and TargetScan to identify the downstream target mRNAs with reference to the four DEmiRNAs. In addition, we sought candidate mRNAs that were only shared by the two databases to enhance the veracity of the prediction. The results revealed that 373 out of 8,294 DEmRNAs were identified. Finally, a total of 5 lncRNAs (4 upregulated and 1 downregulated), 4 miRNAs (1 upregulated and 3 downregulated), and 372 mRNAs (326 upregulated and 46 downregulated) were included to form the HCC-associated lncRNA-miRNAmRNA triple regulatory network by using Cytoscape software (Figure 4A).

The Cytoscape plug-in cytoHubba was utilized to determine the hub triple regulatory network. The results showed that three lncRNAs (DLEU2L, FAM99A, and ARRDC1-AS1), four miRNAs (miR-99a-5p, miR-100-5p, miR-9-5p, and miR-125b-5p), and six mRNA (TAOK1, HS3ST3B1, RHOQ, AGO2, BAZ2A, and NR6A1) were identified (see Figure 4B).

To further explore the potential functions associated with the triple regulatory network, functional enrichment analysis (including GO and KEGG) was utilized by Metascape. The results showed that the DEmRNAs participating in the network were particularly enriched in the "protein kinase activity," "cell morphogenesis involved in differentiation," and "GTPase binding" (Figure 4C).

Construction and validation of the ceRNA network and selection of a model with HCC-specific prognostic value

To establish a crucial ceRNA of great prognostic value in HCC, we first analyzed the expression levels of RNAs from the hub triple regulatory network in HCC samples with PTEN^{high} and PTEN^{low} expression groups and in HCC and adjacent normal liver tissues.
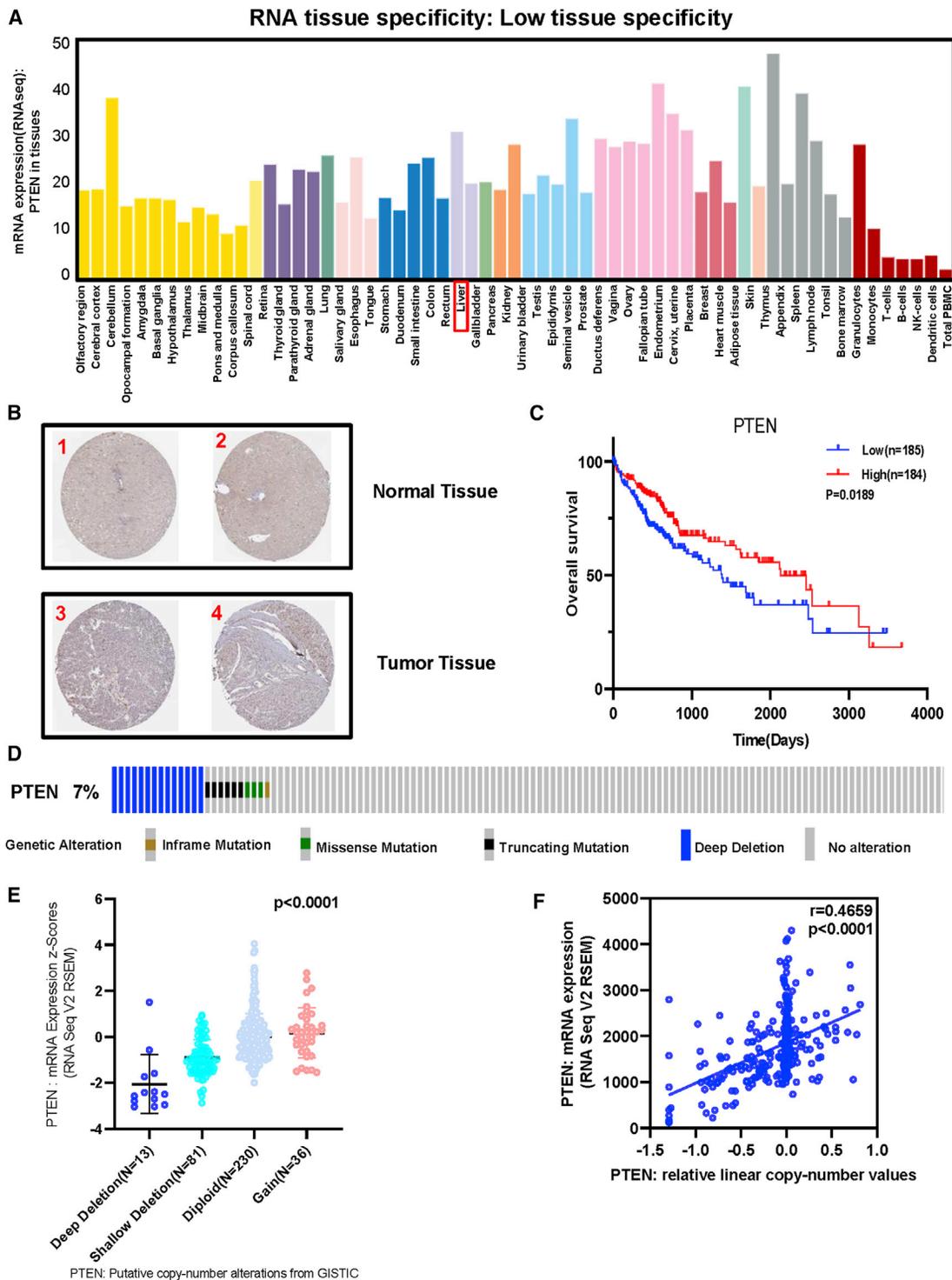
Figure 2. The tumor suppressor role of PTEN in human hepatocellular carcinoma (HCC)

(A) Expression distribution of PTEN in pan-cancer tissues. (B) Validation of the expression of PTEN on the translational level by the Human Protein Atlas database (immunohistochemistry). (C) The low (n = 185) and high expression (n = 184) of PTEN were compared using a Kaplan-Meier survival curve. (D) The distribution of PTEN genomic alterations in TCGA HCC is shown on a cBioPortal OncoPrint plot. (E and F) The association between PTEN copy number and mRNA expression are shown in the dot plot (E) and correlation plot (F) by cBioPortal.
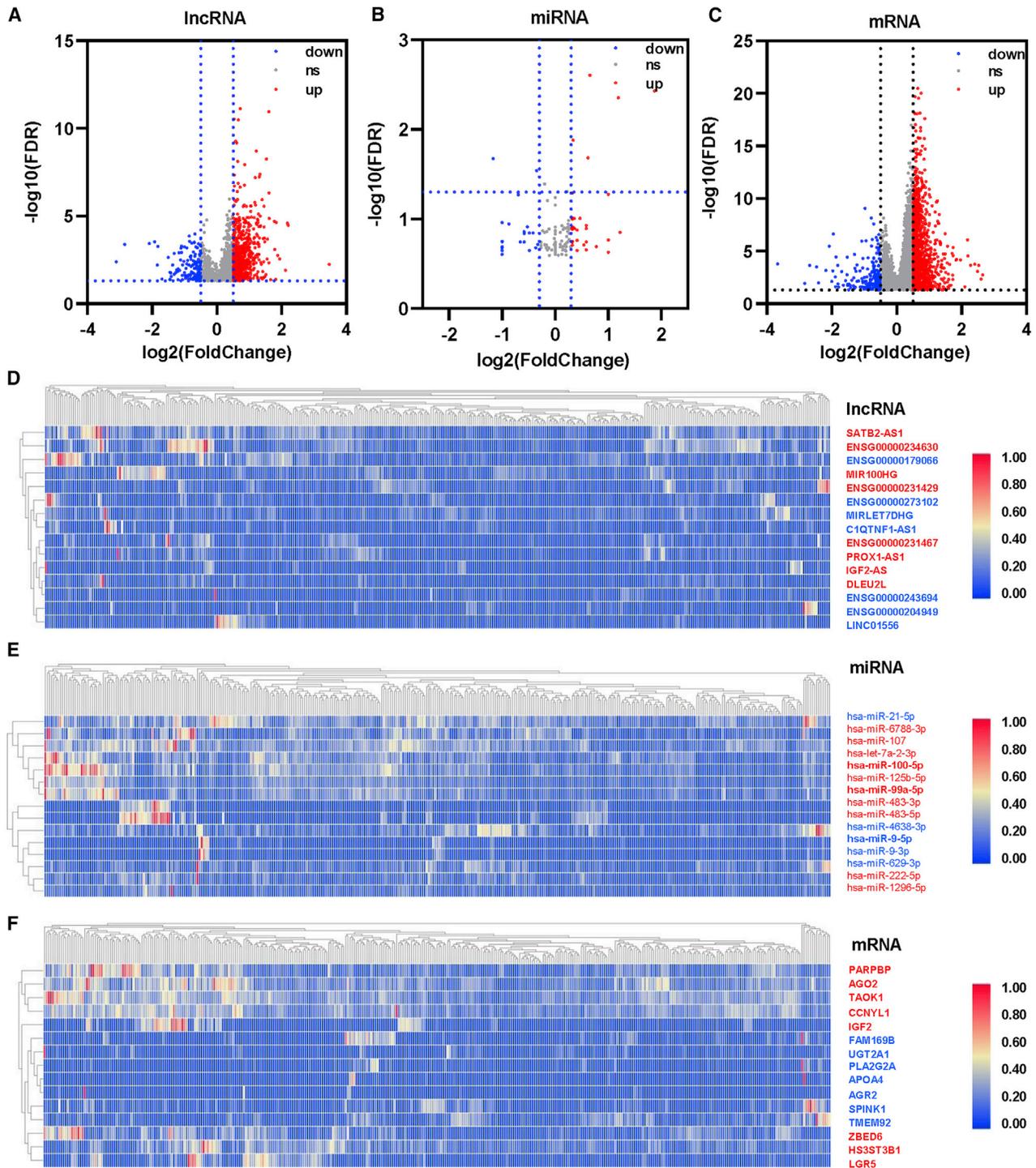
Figure 3. Volcano plots and heatmap plots of DElncRNAs, DEmiRNAs, and DEmRNAs between the expression of PTEN[high] and PTEN[low] in HCC samples
Red represents upregulated genes and blue indicates downregulated genes. (A–C) The volcano plots describe (A) 860DElncRNAs (|log$_2$fold change| > 0.5 and adjusted p value < 0.05), (B) 54DEmiRNAs (|log$_2$fold change| > 0.3 and adjusted p value < 0.05), and (C) 1871DEmRNAs (|log$_2$fold change| > 0.5 and adjusted p value < 0.05). (D–F) The horizontal axis of the heatmap indicates the samples, and the vertical axis of the heatmap indicates 15 significant DEGs.
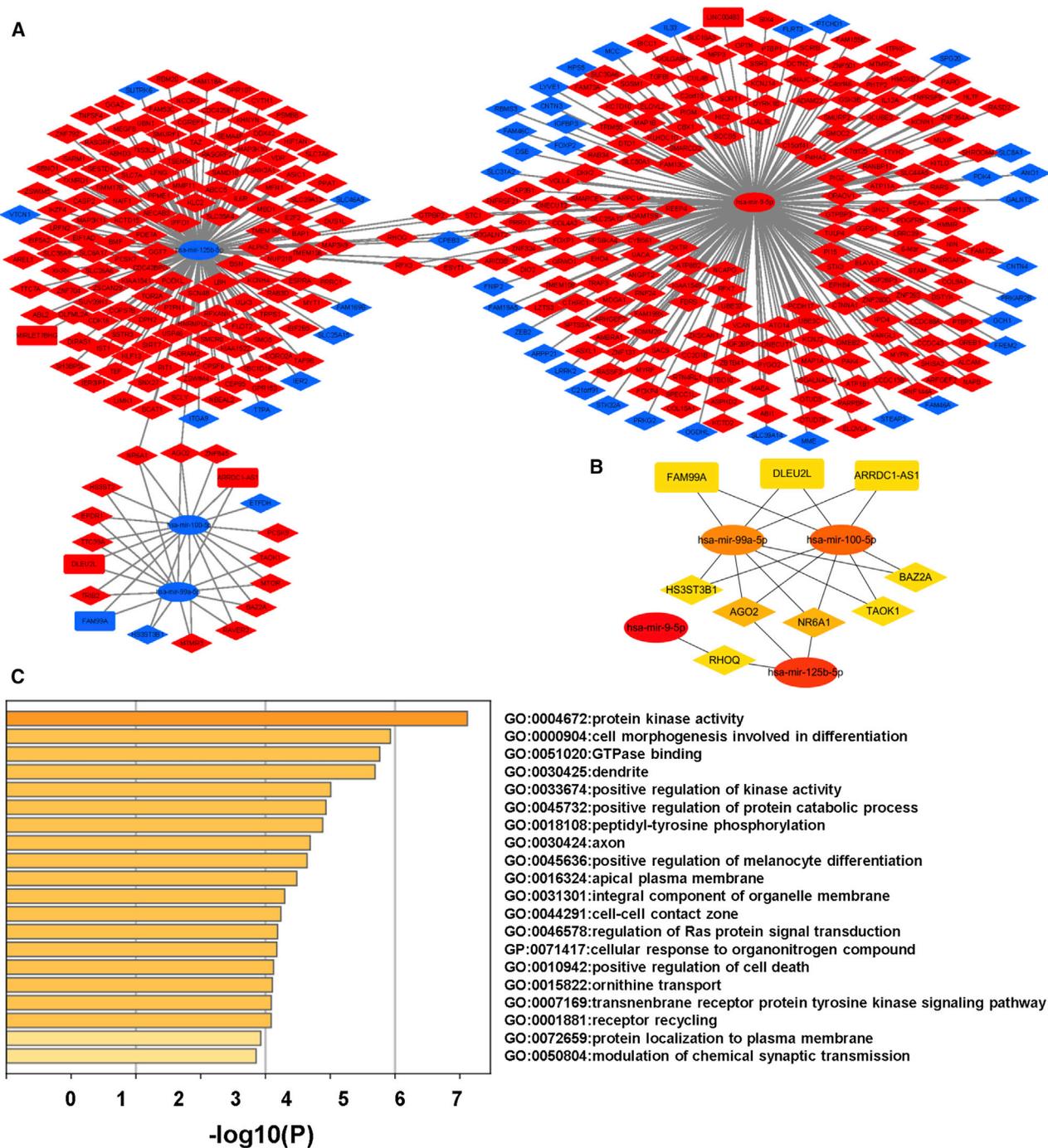
Figure 4. Construction and functional enrichment analysis of the lnRNA-miRNA-mRNA triple regulatory network

The ellipses denote miRNAs, diamonds denote mRNAs, and round rectangles denote lncRNAs. (A) The triple regulatory network in HCC. Red indicates upregulated, and blue represents downregulated. (B) Thirteen hub genes in this network with a score of >2. (C) Functional enrichment analysis (GO and KEGG) of the DEmRNAs in the network

As mentioned above, the expression levels in HCC samples with PTEN^{high} and PTEN^{low} expression groups are opposite to those in cancer and paracancerous groups. Our results showed one downregulated (DLEU2L) and two undifferentiated (ARRDC1-AS1 and FAM99A) lncRNAs, one upregulated (miR-9-5p) and three downregulated (miR-99a-5p, miR-100-5p, and miR-125b-5p) miRNAs, three downregulated (TAOK1, HS3ST3B1, and AGO2) and three undifferentiated (RHOQ, BAZ2A, and NR6A1)
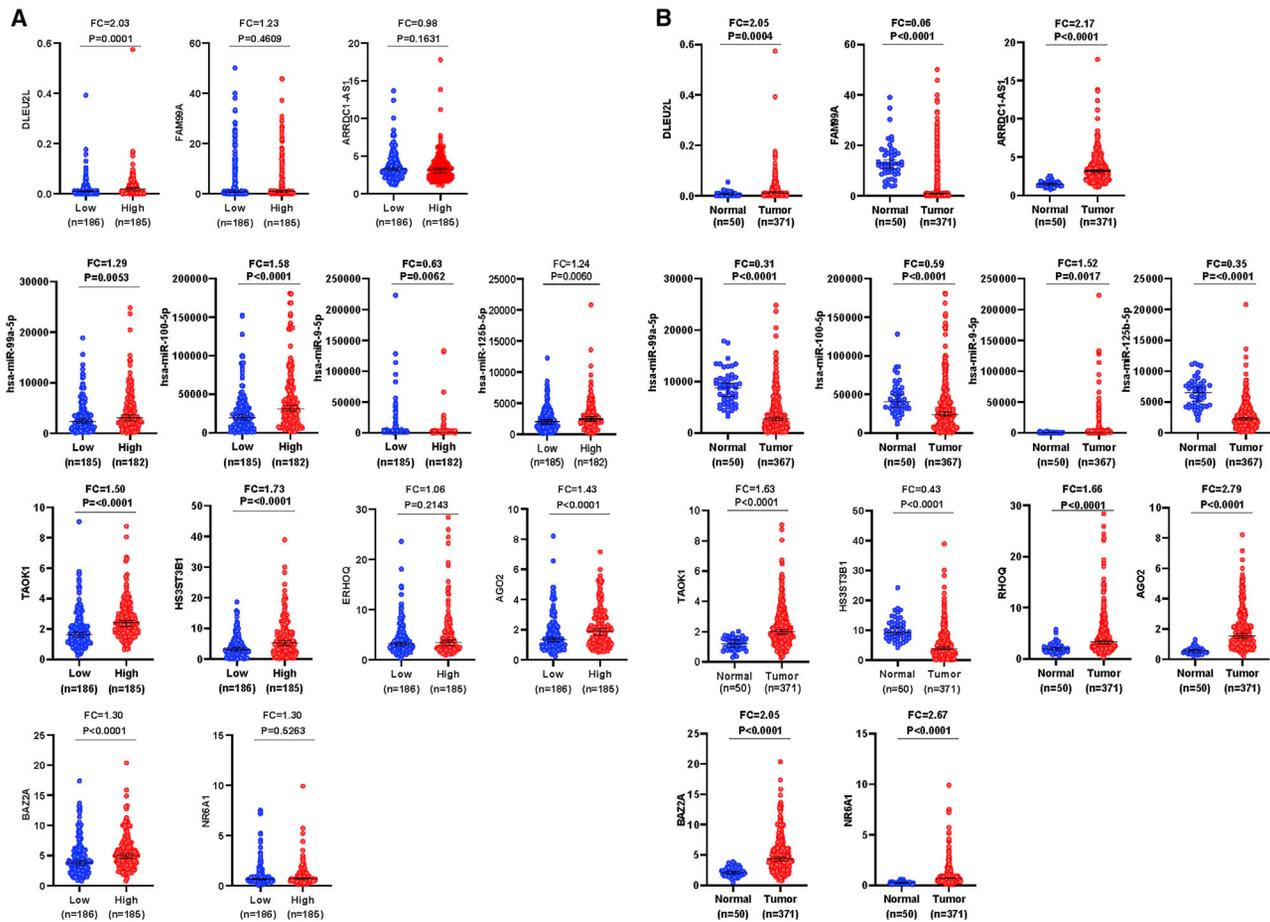
Figure 5. The distribution of 13 hub-RNA expression patterns from the triple regulatory network in TCGA HCC dataset
(A and B) The expression patterns of three hub-DElncRNAs, four hub-DEmiRNAs, and six hub-DEmRNAs in HCC samples with PTEN^high and PTEN^low expression groups (A), and in HCC and adjacent normal liver tissues (B).

mRNAs in HCC samples with PTEN^high and PTEN^low expression groups (Figure 5A), while we found two upregulated (DLEU2L and ARRDC1-AS1) and one downregulated (FAM99A) lncRNAs, one upregulated (miR-9-5p) and three downregulated (miR-99a-5p, miR-100-5p, and miR-125b-5p) miRNAs, and five upregulated (TAOK1, RHOQ, AGO2, BAZ2A, and NR6A1) and one downregulated (HS3ST3B1) mRNAs in HCC and adjacent normal liver tissues (Figure 5B).

Additionally, the expression levels of these RNAs were verified in 50 paired HCC samples from TCGA cohort. An almost consistent finding with the above analysis was elucidated (Figure S3).

Then, to determine whether these RNAs were associated with HCC prognosis, we used Kaplan-Meier analysis and a log-rank test to perform OS analysis of HCC patients. In total, one DElncRNA (DLEU2L), two DEmiRNAs (miR-99a-5p and miR-100-5p), and three DEmRNAs (TAOK1, HS3ST3B1, and RHOQ) were found to be related to prognosis based on p <0.05 (Figure 6).

Moreover, considering that cellular localization of lncRNAs determined the underlying mechanisms, we analyzed the subcellular localization of the three DElncRNAs by performing the lncLocator. As shown in Figure 7A, DLEU2L was mainly located in the cytoplasm, but the other two lncRNAs (FAM99A and ARRDC1-AS1) were mainly distributed in the cytosol. These data indicate that DLEU2L may act as a ceRNA to improve the expression of TAOK1 through sponging miR-99a-5p/miR-100-5p. Thus, a DLEU2L-miR-100-5p/miR-99a-5p-TAOK1 ceRNA network was constructed (Figure 7B). The target sites in the DLEU2L and TAOK1 3′ UTRs were predicted to pair with miR-99a-5p and miR-100-5p by TarBase and TargetScan, respectively (Figure 7C).

Furthermore, expression correlation analysis indicated a positive relationship between DLEU2L expression and TAOK1 expression (Figure 7D). Therefore, the DLEU2L/TAOK1 axis in the ceRNA network was selected as a potential prognostic model for the following step analysis.
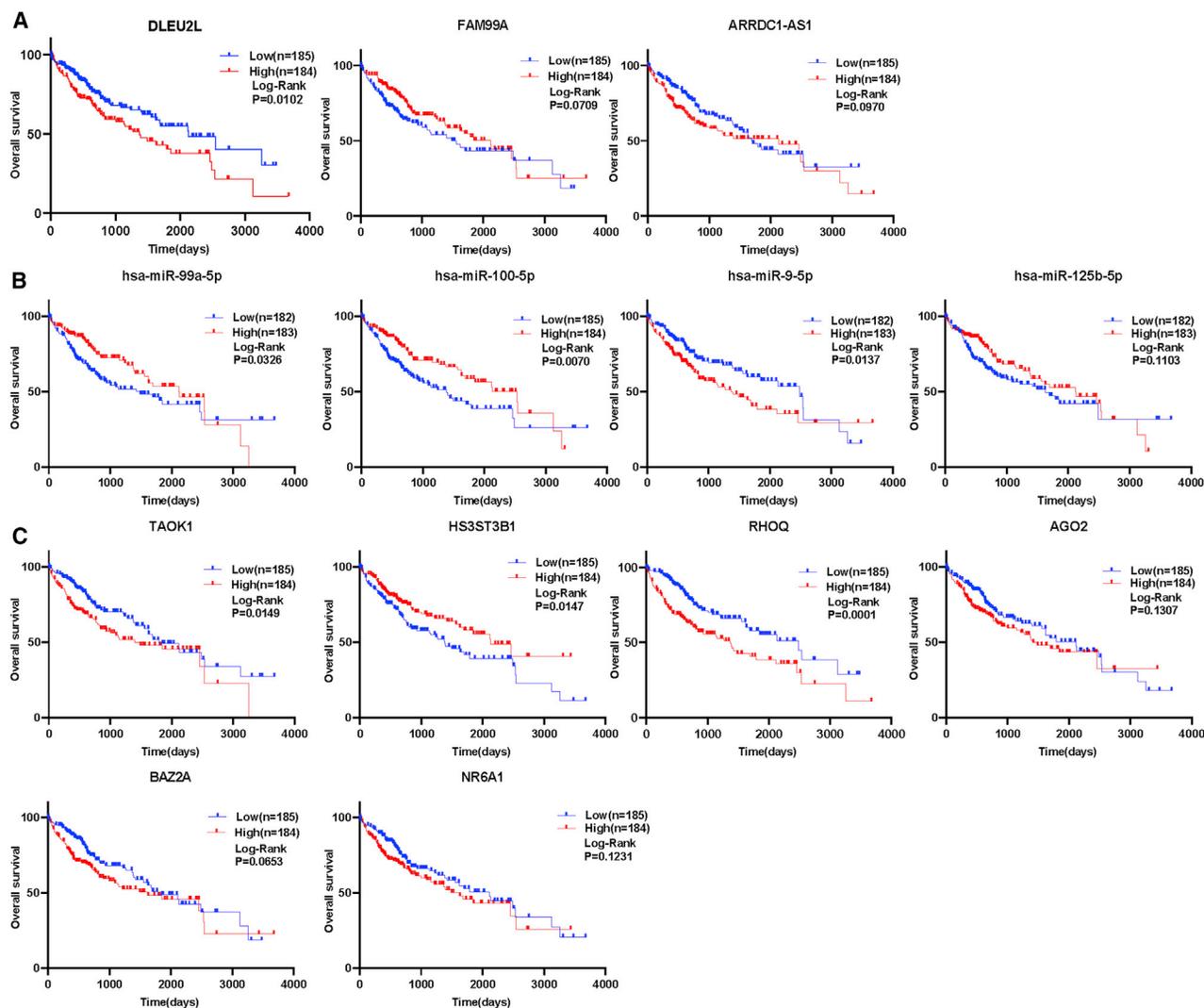
Figure 6. Overall survival analysis for the RNAs in the hub triple regulatory network

(A–C) The high- and low-expression values of three hub-lncRNAs (A), four hub-miRNAs (B), and six hub-mRNAs (C) were compared by a Kaplan-Meier survival curve for TCGA HCC patient cohort. The horizontal axis indicates the overall survival time in days, and the vertical axis represents the survival rate.

Clinical relevance of the DLEU2L/TAOK1 axis in HCC Patients

To determine whether the expression levels of DLEU2L and TAOK1 were affected by clinical characteristics, we explored the correlation of DLEU2L expression and TAOK1 expression with clinical factors. Our study demonstrated that both DLEU2L and TAOK1 expression levels were positively correlated with the diameter of the tumor (DLEU2L, p = 0.031; TAOK1, p = 0.029) and tumor-node-metastasis (TNM) stage (DLEU2L, p = 0.048; TAOK1, p = 0.032), as shown in Table S2. However, we did not observe any association between the expression levels of DLEU2L and TAOK1 and age, sex, lymph node metastasis, distant metastasis, and BMI (p > 0.05; Table S2)

To further analyze the prognostic significance of clinical features, we conducted univariate and multivariate Cox regression analyses to determine OS-related features. In univariate Cox regression analysis models of DLEU2L and TAOK1, some prognostic factors (TNM stage, tumor diameter, lymph node metastasis, and distant metastasis) were closely relevant to OS (p < 0.05; Tables S3 and S4) in HCC patients in TCGA cohorts.

Importantly, both DLEU2L (hazard ratio [HR] = 1.572, p = 0.011) and TAOK1 (HR = 1.537, p = 0.016) overexpression levels were significantly associated with a worse prognosis (Table S4). In multivariate Cox regression analysis of TAOK1, tumor diameter (HR = 2.245, p = 0.000), distant metastasis (HR = 1.325, p = 0.003), and TAOK1^{high} expression (HR = 1.622, p = 0.007) were still relevant to OS (Table S4) in HCC patients. However, multivariate Cox regression analysis of DLEU2L revealed that elevated DLEU2L expression was
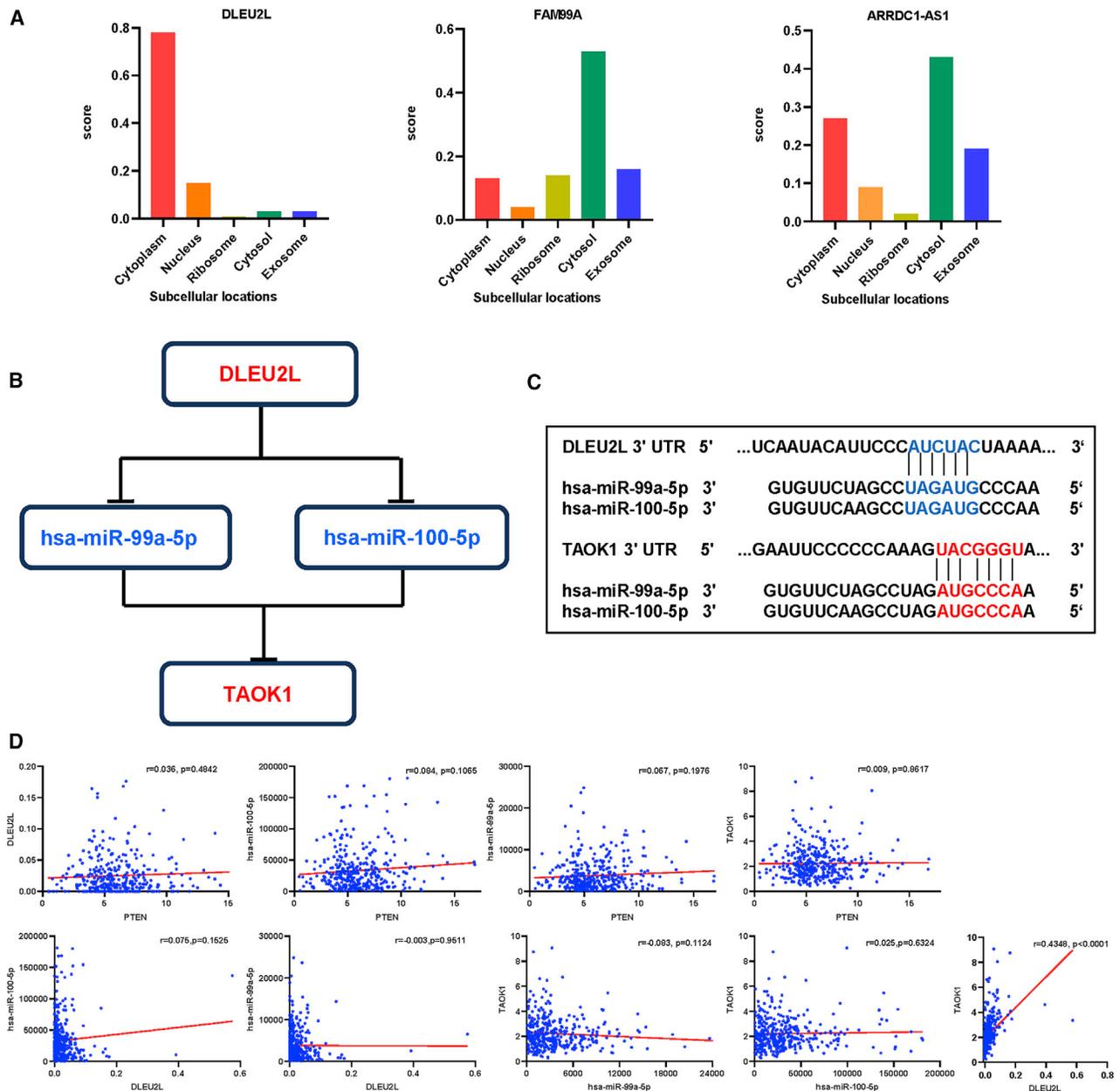
Figure 7. Construction and correlation analysis of the ceRNA network

(A) The cellular localization for three hub-lncRNAs (DLEU2L, FAM99A, and ARRDC1-AS1) was predicted using lncLocator. (B) Schematic model of ceRNA. Blue indicates downregulated; red indicates upregulated. (C) Base pairing between miR-99a-5p and miR-100-5p and the target site in the DLEU2L and TAOK1 3′ UTR predicted by TarBase and TargetScan, respectively. (D) Correlation analysis between these four predictive RNAs and PTEN in HCC.

not correlated with a poor prognosis (HR = 1.369, p = 0.078; Table S3). Thus, TAOK1 may become an independent prognostic factor for HCC patients.

Validation of TAOK1 abnormally high expression

For the sake of better understanding the role of the DLEU2L/TAOK1 axis in HCC, we next analyzed TAOK1 in detail. First, based on the online tool Cancer Cell Line Encyclopedia (CCLE), we found that

TAOK1 was high expression in HCC cell lines (Figure S4A). Additionally, we performed the difference analysis of TAOK1 in HCC patients with 20 paired HCC samples from the GEO: GSE41804 HCC cohorts in the GEO database to verify the expression of TAOK1 further (Figure S4B). The results revealed that the expression of TAOK1 in the HCC tissues was markedly higher than that of the paired nontumorous liver tissues, which coincided with our results from TCGA data (Figures 5A and 6).

In addition, considering that the genetic mutation might act as a potential mechanism to promote the abnormal overexpression of TAOK1, we performed the following analysis. In Figure S5A, an OncoPrint plot shows the amplification of TAOK1 gene in TCGA HCC dataset. However, no significant associations were observed for TAOK1 expression and copy number values among HCC samples (Figures S5B and S5C). Hence, these data demonstrated no correlation between TAOK1 abnormal expression and copy number alterations in HCC.

Relationship between methylation and expression of TAOK1

To further elucidate the abnormal upregulated mechanisms of TAOK1 in HCC tissues, we also explored the correlation of TAOK1 expression levels and their methylation status by various methods. First, differential expression analysis of three DNA methyltransferases (DNMT1, DNMT3A, and DNMT3B) between TAOK1^{high} and TAOK1^{low} groups of HCC showed that expression of the DNMT1, DNMT3A, and DNMT3B in TAOK1^{high} group was markedly increased compared with that in TAOK1^{low} group (Figure 8A). Second, the analysis of UALCAN showed that DNMT1 had a trend of higher methylation level in normal liver tissues than in HCC tissues (p = 0.101, Figure 8B). Similarly, DiseaseMeth version 2.0 analysis demonstrated that the methylation of TAOK1 was significantly higher in paracancerous normal tissues compared with HCC tissues (p < 0.0001; Figure 8C). Additionally, we found two methylation sites (cg16008158 and cg2570978) in the DNA sequences of TAOK1 that were negatively associated with their expression levels (Figure 8D). Third, the differential methylation regions related to TAOK1 were presented as heatmaps (Figure S6). Interestingly, a NEURL1B-associated methylation site cg2570978 was found in the open sea region and 3′ UTR region (Figure S6).

Correlation between immune infiltration and expression of TAOK1 in HCC

It has been reported that tumor-infiltrating lymphocytes (TILs) are independent predictors of sentinel lymph node (SLN) status and survival in certain cancers.[37] To evaluate the potential relationship between TAOK1 expression and immune infiltration levels in HCC, we conducted the following analysis by using TIMER. First, the "SCNA" module analysis showed that several immune cell infiltration levels seemed to associate with altered TAOK1 gene copy numbers, including B cells, CD4$^+$ T cells, macrophages, and dendritic cells (DCs) in HCC (Figure 9A). Then, the "Gene" module analysis showed that TAOK1 expression has no notable correlation with tumor purity, but it is markedly positively correlated with infiltrating levels of CD4$^+$ T cells, macrophages, neutrophils, and dendritic cells in HCC (Figure 9B). Finally, we further evaluated the impact of immune infiltration on the clinical prognosis of patients with HCC.

The results showed that high levels of CD4$^+$ cells, macrophages, and neutrophils were associated with poor prognosis of HCC patients with a survival period of less than 24 months (p = 0.036, 0.007, and 0.01, respectively). These results indicate that the DLEU2L/TAOK1 axis may affect HCC and clinical prognosis by regulating the level of tumor-infiltrating immune cells.

To further validate the relationship between TAOK1 and diverse immune-infiltrating cells, we also explored the associations between TAOK1 and immune marker sets of 16 immune cells.[38] Interestingly, we found that the expression levels of five markers (BDCA-4 [NRP1], STAT1, STAT6, STAT3, and STAT5B) of dendritic cells, T helper (Th)1, Th2, Th17, and regulatory T cells (Tregs) have markedly positive correlations with LAYN expression in HCC (Tables S5 and S6).

We also investigated the relationship between TAOK1 expression and the above markers of dendritic cells, Th cells (Th1, Th2 and Th17), and Tregs in the GEPIA database in HCC. Correlation analysis results showed a similar trend to TIMER (Tables S5 and S6). These results suggest that tumor-infiltrating immune cells may have an influence on the clinical outcome of the DLEU2L/TAOK1 axis in HCC.

TAOK1-related functional enrichment analysis in HCC

To further investigate the possible function of TAOK1 in HCC, we utilized GO and KEGG pathway enrichment analysis of the top 200 correlated genes of TAOK1 in HCC (Figure S7). The enrichment term related to TAOK1 is the mitogen-activated protein kinase (MAPK) signaling pathway. Moreover, GO enrichment analyses, including biological process (BP), cellular component (CC), and molecular function (MF), related to TAOK1 were mainly enriched in "mitotic cell cycle phase transition," "histone modification," and "kinase activity."

DISCUSSION

HCC is one of the leading causes of cancer mortality worldwide due to its poor prognosis and high aggressiveness.[39–42] Although various therapeutic strategies have been adopted for HCC patients, the prognosis is still poor.[43–46] Clarifying the molecular mechanisms and processes of the pathogenesis of HCC and identifying promising biomarkers are essential for identifying new therapeutic targets and improving patients' outcome with this disease.[47–49] According to reports, the ceRNA regulatory network participates in the occurrence and development of many human cancers, including lung cancer,[50] gastric cancer,[51] and pancreatic cancer.[52] However, to our knowledge, few studies have focused on a comprehensive ceRNA regulatory network to predict the prognosis of HCC. Accordingly, in this study, we attempted to establish a PTEN-related ceRNA triple network in HCC, as well as associate it with prognosis. Increasing evidence has demonstrated that PTEN acts as a tumor suppressor functionally involved in many types of cancers, including HCC.[53–55] Interestingly, we verified similar results in this study through survival analysis, IHC, and copy number variation analysis.

In this study, first, the lncRNA-miRNA-mRNA triple regulatory network containing 5 lncRNAs, 4 miRNAs, and 372 mRNAs was obtained through in silico analysis. Enrichment analysis showed that the network was mainly concentrated in "protein kinase activity," "cell morphogenesis involved in differentiation" and "GTPase binding."
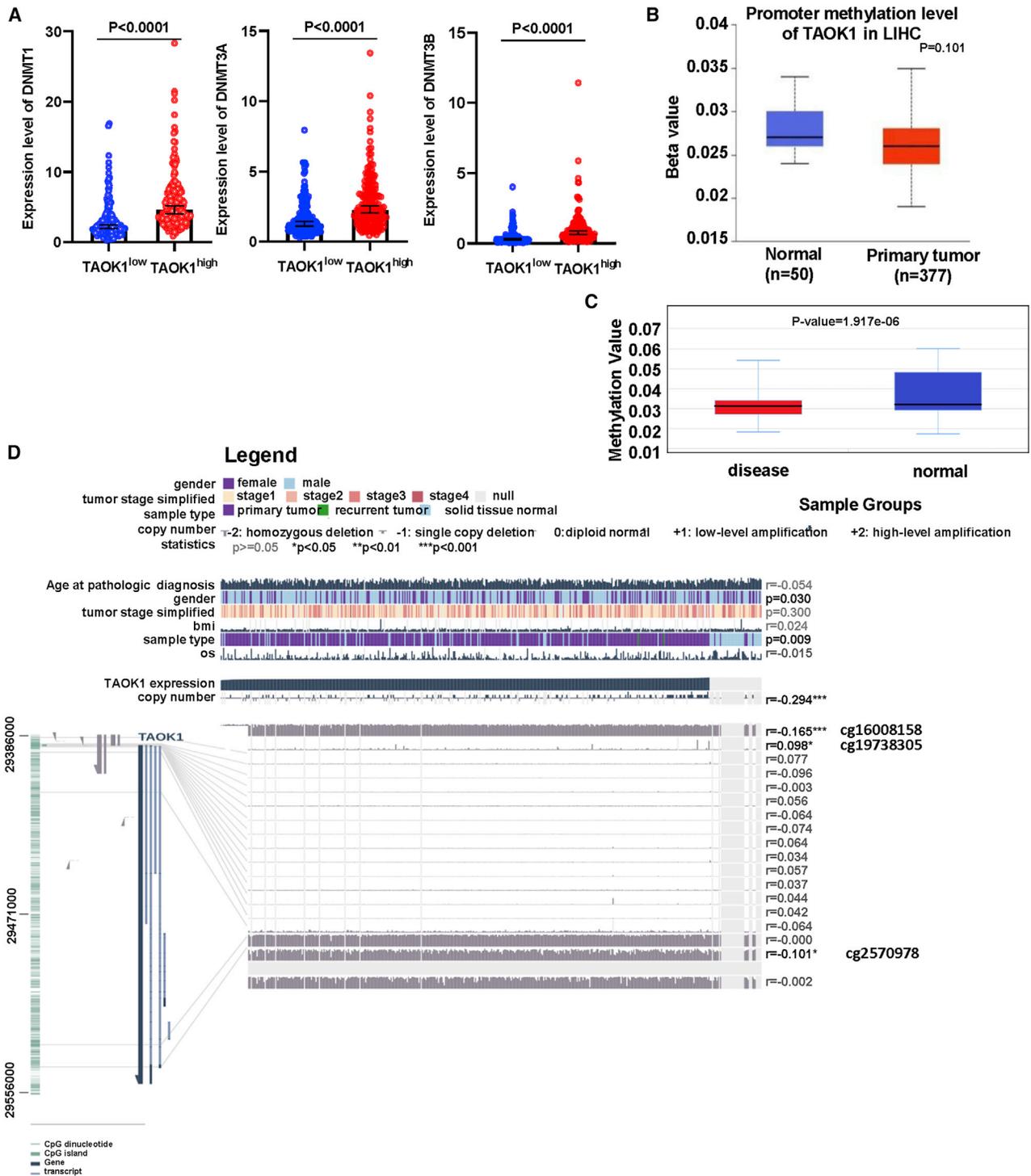
Figure 8. Methylation analysis of TAOK1

(A) Differential expression of three DNA methyltransferases (DNMT1, DNMT3A, and DNMT3B). (B) Methylation was evaluated using UALCAN. (C) Methylation was assessed using DiseaseMeth version 2.0. (D) The methylation site of TAOK1 DNA sequence association with gene expression was visualized using MEXPRESS. The expression of TAOK1 is illustrated by the blue line in the center of the plot. Pearson's correlation coefficients and p values for methylation sites and query gene expression are shown on the right side.
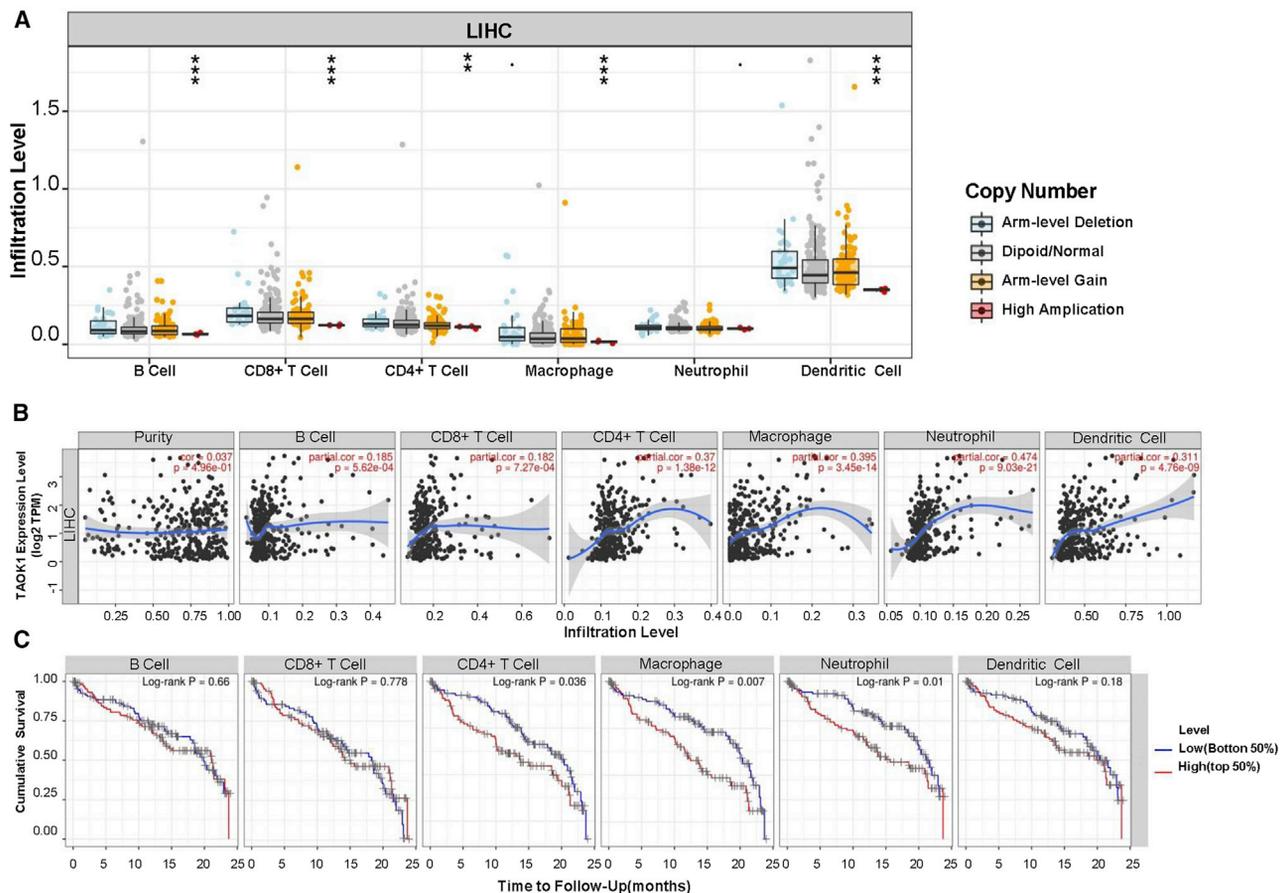
Figure 9. Correlation analysis of TAOK1 expression and immune infiltration in HCC

(A) Association between TAOK1 gene copy number and immune cell infiltration levels in HCC cohorts. (B) Correlation of TAOK1 expression with immune infiltration level in HCC. (C) Kaplan-Meier plots were used to analyze the immune infiltration and overall survival rate of HCC. *p < 0.05, **p < 0.01, ***p < 0.001.

Next, a key triple regulatory network was obtained by hub analysis based on a score >2, including three lncRNAs, four miRNAs, and six mRNAs. Finally, the expression analysis and survival analysis were performed on this hub regulatory network. Moreover, because the interactions in the ceRNA network exist only in the cytoplasm, we also performed subcellular localization analysis of the three lncRNAs in the network. In summary, the DLEU2L-hsa-miR-100-5p/ hsa-miR-99a-5p-TAOK1 overexpressed ceRNA network related to the prognosis of HCC was obtained.

By searching for these genes in PubMed, we observed that miR-100-5p, miR-99a-5p, and TAOK1 have been studied for their roles in cancer or in the relationship with cancer. Stroese et al.[56] provided results suggesting that the miRNA-99 family is an unfavorable prognostic factor for patients with pancreatic ductal adenocarcinoma (PDAC), and Dhayat et al.[57] performed bioinformatics analysis and concluded that miR-99a upregulation is involved in the control of PDAC cell death and cycle pathways. However, we found that the low expression of miR-99a-5p is related to the poor prognosis of breast cancer, lung adenocarcinoma, cervical cancer,[58] and similar

phenomena in HCC.[59] Song et al.[60] study showed that low expression of miR-100-5p was relevant to gross vascular invasion (VI) and worse outcome of HCC patients after hepatic resection. Additionally, another study suggested that miR-100 inhibits the migration and invasion of nasopharyngeal carcinoma cells by targeting insulin-like growth factor 1 receptor.[61] Agosto-Arroyo et al.[62] found that the overexpression of TAOK1 in the ERBB2 subtype could be associated with the occurrence of invasive breast cancer. Thean et al.[63] have concluded that TAOK1 as a target oncogene of miR-24 was coordinately upregulated with PIM2 and MIA-RAB4B to contribute to colorectal cancer. However, according to searches in PubMed, few studies have investigated the role of DLEU2L in cancer.

In our study, DLEU2L and TAOK1 expression were significantly higher in HCC than in normal tissues, and high expression of DLEU2L and TAOK1 was associated with poor outcome by survival analysis. Opposite to DLEU2L and TAOK1, miR-100-5p and miR-99a-5p expression were downregulated, and the low expression level of IGF2BP1 indicated worse OS prognosis in HCC.

In the current study, we found no correlation between TAOK1 abnormal overexpression and copy number alterations in HCC. According to research, DNA methylation plays an important role in regulating gene expression.[64–67] Therefore, we referred to some websites to explore DNA methylation patterns that could account for the abnormal expression of TAOK1 in HCC. We found that TAOK1 was hypomethylated in HCC samples compared with adjacent normal ones, which is consistent with the observed upregulation of TAOK1 in HCC combined with DNA methyltransferase analysis (DNMT1, DNMT3A and DMNT3B). We also found that the TAOK1^{high} group clearly co-occurred with higher expression of DNMT1, DNMT3A, and DNMT3B, which promoted us to understand the upregulated expression of NEURL1B in HCC. Additionally, we found a negative correlation between some methylated sites and the prognosis of HCC patients. Finally, associations between TAOK1 expression and genome-wide methylation were exploited. The results showed that more hypermethylation sites were nearer to the open sea regions (Figure 5C). Moreover, all hypermethylated sites fell in UTR regions (3′ UTR and 5′ UTR), while more hypomethylation sites were in the TSS1500 and TSS200 regions. Importantly, the NEURL1B-associated methylation site cg2570978 was in the open sea region and 3′ UTR region. These findings suggest that the abnormal methylation may be related to HCC poor prognosis.

Previous studies have reported that immune infiltration can affect the prognosis of the patient.[68–70] In this study, we found that TAOK1 gene copy numbers were inversely associated with the infiltration levels of B cells, CD8^{+} T cells, CD4^{+} T cells, macrophages, neutrophils, and dendritic cells in lung cancer by using TIMER. The immune cell infiltration levels changed along with the ACK1/TNK2 gene copy numbers. We found that several immune cell infiltration levels (B cells, CD8^{+} T cells, CD4^{+} T cells, macrophages, and dendritic cells) were inversely correlated with TAOK1 gene copy numbers in HCC. We also found that the expression of TAOK1 was highly correlated with immune infiltration of HCC. Additionally, several types of tumor-infiltrating immune cells were notably related to the prognosis of HCC patients.[71–75] Furthermore, significant positive correlations were revealed between TAOK1 expression and some immune marker sets in dendritic cells, Th cells (Th1, Th2, and Th17) and Tregs in HCC. These findings together suggest that these differences induced by the DLEU2L/TAOK1 axis may have an impact on the changes in the tumor immune microenvironment and the development of HCC.

To further explore the biological functions of TAOK1, we conducted GO and KEGG enrichment analyses for TAOK1. The enrichment term related to TAOK1 is MAPK signaling pathway. GO enrichment analysis (including BP, CC, and MF) related to TAOK1 mainly enriched in mitotic cell cycle phase transition, histone modification, and kinase activity.

Although we have constructed the ceRNA-based DLEU2L/TAOK1 axis, which appears to be a potential prognostic biomarker in clinical applications, several limitations must also be noted. First, the binding affinity of lncRNAs, miRNAs, and mRNAs obtained from the database should be further experimentally investigated. Second, we need to further study the function and mechanism of the DLEU2L/TAOK1 axis in HCC by experiments.

In conclusion, we established a ceRNA (DLEU2L-hsa-miR-100-5p/hsa-miR-99a-5p-TAOK1) overexpressed network related to the prognosis of HCC, which is better for knowing the correlation among lncRNA-miRNA-mRNA. Additionally, we identified that the ceRNA-based DLEU2L/TAOK1 axis can be a novel significant prognostic factor participating in HCC, and the prognostic model is useful for exploring the pathogenesis of HCC.

MATERIALS AND METHODS
Data preparation and processing
Figure 1 shows the workflow chart of this study. We downloaded primitive data (expressing profiles) and clinic information of human HCC from TCGA database (https://portal.gdc.cancer.gov/). Available mRNA sequencing (mRNA-seq) data for 371 HCC samples (including 50 paired HCC samples) and miRNA sequencing (miRNA-seq) data from 367 HCC samples (including 50 paired HCC samples) were gained from TCGA database. All raw RNA-seq data (lncRNAs, miRNAs, and mRNAs) were normalized as fragments per kilobase of exon model per million mapped fragment reads. Transformation of miRNA sequences into human mature miRNA names was accomplished using the starBase version 2.0 database (http://starbase.sysu.edu.cn).

Meanwhile, we also downloaded the gene expression profiles from GEO: GSE41804 (including 20 HCC samples and 20 adjacent nontumor samples; platform, GEO: GPL570), which were extracted from the GEO database (https://www.ncbi.nlm.nih.gov/geo/), to further validate our results. CCLE (https://portals.broadinstitute.org/ccle) and HPA (http://www.proteinatlas.org/) searches were performed to verify the expression of PTEN and TAOK1 in HCC cell lines and at the protein level. We obtained the mutation status of PTEN and TAOK1 through the cBioPortal for Cancer Genomics (http://www.cbioportal.org/).

Screening of DEGs
When performing the differential expression analysis in PTEN[high] and PTEN[low] HCC samples, we determined the DElncRNAs with thresholds of $|logFC| > 0.5$ and $p < 0.05$, the DEmiRNAs with thresholds of $|logFC| > 0.3$ and $p < 0.05$, and the DEmRNAs with thresholds of $|logFC| > 0.5$ and $p < 0.05$. When performing differential expression analysis between HCC samples and adjacent nontumorous samples, the critical value of DElncRNAs was set to $p < 0.05$ and $|logFC| > 0.5$, the critical value of DEmiRNAs was set to $p < 0.05$ and $|logFC| > 0.3$, and the critical value of DEmRNAs was set to $p < 0.05$ and $|logFC| > 0.7$. Volcano plots of the DERNAs (including DElncRNAs, DEmiRNAs, and DEmRNAs) were visualized using GraphPad Prism 8 software (version 8.3.0). The heatmap clustering was drawn by TBtools software (version 1.051).

Establishment of the ceRNA network in HCC

According to the hypothesis that lncRNA could indirectly regulate mRNA expression by competing with miRNA as a natural sponge in the cytoplasm, the ceRNA network was constructed by the following steps: (1) TarBase (TarBase v7.0 database, http://microrna.gr/tarbase/) was used to predict the potential miRNAs targeted by DElncRNAs and the lncRNA-miRNA interaction pairs; (2) miRDB (http://www.mirdb.org/) and TargetScan (version 7.2, http://www.targetscan.org/) were used to forecast the target genes of the DEmiRNAs and build the miRNA-mRNA interaction pairs; (3) the VennDiagram package in R software was utilized to compare the target genes with DEmRNAs, and the target genes that overlapped with DEmRNAs in this study were selected for the next analysis; and (4) by integrating the lncRNA-miRNA pairs with miRNA-mRNA pairs, we built the lnRNA-miRNA-mRNA triple regulatory network.

LNCipedia (https://lncipedia.org/) was used to obtain DElncRNA sequences, and the lncLocator (http://www.csbio.sjtu.edu.cn/bioinf/lncLocator/) database was used to identify the DElncRNA cellular localization based on its sequence. The Cytoscape plug-in cytoHubba was performed to identify the hub triple regulatory network. The generated networks were visualized by Cytoscape software (version 3.7.0, https://www.cytoscape.org/).

Functional enrichment analysis

For the sake of understanding the possible biological processes and pathways of the network, we conducted the following analysis. To begin with, we conducted a functional enrichment analysis of the DEmRNAs in the lncRNA-miRNA-mRNA triple regulatory network in Metascape (http://metascape.org/gp/index.html). Then, the top 200 TAOK1-associated genes in LIHC was obtained from GEPIA (http://gepia.cancer-pku.cn/), and GO enrichment (including BP, CC, and MF) and KEGG pathway analyses of these genes were performed using Metascape and visualized by the R package ggplot2. An adjusted $p < 0.05$ was determined to be statistically significant.

Survival analysis and construction of a specific prognosis model for HCC

The survival status and time of HCC patients were gained from TCGA clinical dataset. We used GraphPad Prism 8 software to perform Kaplan-Meier analysis and a log-rank test on DElncRNAs, DEmiRNAs, and DEmRNAs in the ceRNA network to determine the relationship with the OS of HCC patients in TCGA database. Univariate Cox regression analysis was utilized to analyze the association between candidate genes in the ceRNA network and OS to determine the prognostic-related biomarkers. Multivariate Cox regression analysis was performed on TAOK1 to determine the independent prognostic factors of HCC. A log-rank $p < 0.05$ was determined to be statistically significant.

Methylation and expression analysis of TAOK1

Studies showed that DNA methylation is a significant epigenetic mechanism, which is able to regulate gene expression by three DNA methyltransferases (DNMT1, DNMT3A, and DNMT3B) and influence the behavior of cancer cells. First, we investigated the expression level of three DNA methyltransferases in TAOK1^{high} and TAOK1^{low} groups by TCGA database. Then, we utilized the human disease methylation database DiseaseMeth version 2.0 (http://bio-bigdata.hrbmu.edu.cn/diseasemeth/) and UALCAN (http://ualcan.path.uab.edu/) to assess methylation levels of TAOK1 between the HCC and paracancerous normal tissues. Moreover, we investigated the association between hub genes' expression and their DNA methylation status using MEXPRESS (https://mexpress.be). Finally, MethSurv (https://biit.cs.ut.ee/methsurv/) was used to perform multivariate survival analysis to evaluate the scattering of different CpG islands.

Immune infiltrate levels and expression analysis of TAOK1

To investigate the association of the expression of TAOK1 and tumor-infiltrating immune cells, we applied TIMER (https://cistrome.shinyapps.io/timer/), which is an online tool for the analysis and visualization of the correlation between immune infiltrate levels and a number of variables across diverse cancer types. We explored the correlation of TAOK1 expression with the abundance of tumor-infiltrating immune cells (including B cells, CD4$^+$ T cells, CD8$^+$ T cells, neutrophils, macrophages, and dendritic cells), the prognostic value, and TAOK1 copy numbers in HCC.

Furthermore, we estimated the correlation of TAOK1 with the markers of 16 tumor-infiltrating immune cells (including markers of CD8$^+$ T cells, T cells, B cells, monocytes, TAMs, M1 macrophages, M2 macrophages, neutrophils, natural killer [NK] cells, dendritic cells, Th1 cells, Th2 cells, follicular Th [Tfh] cells, Th17 cells, Tregs, and exhausted T cells).

Statistical analysis

The obtained data were analyzed using GraphPad Prism (version 8.0) and SPSS 23.0 software (SPSS, Chicago, IL, USA). The results are presented as the median and 95% confidence interval (CI). The Mann-Whitney test and an independent t test were used to calculate the difference between two groups of data, while a one-way ANOVA with the Kruskal-Wallis test and chi-square test were utilized to evaluate the difference among different groups. $p < 0.05$ was considered as statistically difference.

SUPPLEMENTAL INFORMATION

Supplemental Information can be found online at https://doi.org/10.1016/j.omtn.2020.12.016.

ACKNOWLEDGMENTS

AUTHOR CONTRIBUTIONS

Y.-S.M., D.F., and W.L. designed the study; Y.S., D.-D.Z., J.-B.L., X.-L.Y., R.X., C.-Y.J., H.-M.W., G.-X.L., P.-Y.W., Z.-J.L., Y.-S.M., D.F., and W.L. conducted the study; Y.S., D.-D.Z., Y.L., Z.-J.L., J.D., Q.-L.L., L.M., S.-S.F., X.-Q.C., X.-M.Z., Y.-F.Z., Y.-J.H., H.-Q.Y., L.-L.T., L.-P.G., Z.-W.L., F.Y., Y.-S.M., and D.F. collected data; Y.S, D.-D.Z., Y.-S.M., D.F., and W.L. performed the statistical analyses and interpreted the data; Y.-S.M., D.F., and W.L. contributed to study materials and consumables; and Y.S, Y.-S.M., D.F., and W.L. wrote the manuscript. All authors contributed to the final version of the manuscript and approved the final manuscript.

DECLARATION OF INTERESTS

The authors declare no competing interests.

REFERENCES

1. Li, M., Shao, J., Guo, Z., Jin, C., Wang, L., Wang, F., Jia, Y., Zhu, Z., Zhang, Z., Zhang, F., et al. (2020). Novel mitochondrion-targeting copper(II) complex induces HK2 malfunction and inhibits glycolysis via Drp1-mediating mitophagy in HCC. J. Cell. Mol. Med. 24, 3091–3107.

2. Zhao, B., Ke, K., Wang, Y., Wang, F., Shi, Y., Zheng, X., Yang, X., Liu, X., and Liu, J. (2020). HIF-1α and HDAC1 mediated regulation of FAM99A-miR92a signaling contributes to hypoxia induced HCC metastasis. Signal Transduct. Target. Ther. 5, 118.

3. Li, X., Wang, H., Li, T., Wang, L., Wu, X., Liu, J., Xu, Y., and Wei, W. (2020). Circulating tumor DNA/circulating tumor cells and the applicability in different causes induced hepatocellular carcinoma. Curr. Probl. Cancer 44, 100516.

4. Hou, J., Zhang, H., Liu, J., Zhao, Z., Wang, J., Lu, Z., Hu, B., Zhou, J., Zhao, Z., Feng, M., et al. (2019). YTHDF2 reduction fuels inflammation and vascular abnormalization in hepatocellular carcinoma. Mol. Cancer 18, 163.

5. Chen, Z., Zheng, Z., Feng, L., Huo, Z., Huang, L., Fu, M., Chen, Q., Ke, Y., Yang, J., and Hou, B. (2020). Overexpression of miR-382 sensitizes hepatocellular carcinoma cells to γδ T cells by inhibiting the expression of c-FLIP. Mol. Ther. Oncolytics 18, 467–475.

6. Chen, Z., and Hu, H. (2019). Identification of prognosis biomarkers of prostatic cancer in a cohort of 498 patients from TCGA. Curr. Probl. Cancer 43, 100503.

7. Mi, X., Xu, R., Hong, S., Xu, T., Zhang, W., and Liu, M. (2020). M2 macrophage-derived exosomal lncRNA AFAP1-AS1 and microRNA-26a affect cell migration and metastasis in esophageal cancer. Mol. Ther. Nucleic Acids 22, 779–790.

8. Tang, G.D., Luo, L.Y., Zhang, J.L., Zhai, D.F., Huang, D.Q., Yin, J., Zhou, Q., Zhang, Q., and Zheng, G.P. (2021). lncRNA LINC01057 promotes mesenchymal differentiation by activating NF-κB signaling in glioblastoma. Cancer Lett. 498, 152–164.

9. Tong, Y., Yang, L., Yu, C., Zhu, W., Zhou, X., Xiong, Y., Wang, W., Ji, F., He, D., and Cao, X. (2020). Tumor-secreted exosomal lncRNA POU3F3 promotes cisplatin resistance in ESCC by inducing fibroblast differentiation into CAFs. Mol. Ther. Oncolytics 18, 1–13.

10. Zhang, Y., Huang, Y.X., Wang, D.L., Yang, B., Yan, H.Y., Lin, L.H., Li, Y., Chen, J., Xie, L.M., Huang, Y.S., et al. (2020). lncRNA DSCAM-AS1 interacts with YBX1 to promote cancer progression by forming a positive feedback loop that activates FOXA1 transcription network. Theranostics 10, 10823–10837.

11. Teng, F., Zhang, J.X., Chang, Q.M., Wu, X.B., Tang, W.G., Wang, J.F., Feng, J.F., Zhang, Z.P., and Hu, Z.Q. (2020). lncRNA MYLK-AS1 facilitates tumor progression and angiogenesis by targeting miR-424-5p/E2F7 axis and activating VEGFR-2 signaling pathway in hepatocellular carcinoma. J. Exp. Clin. Cancer Res. 39, 235.

12. Zhou, R., Sun, H., Zheng, S., Zhang, J., Zeng, D., Wu, J., Huang, Z., Rong, X., Bin, J., Liao, Y., et al. (2020). A stroma-related lncRNA panel for predicting recurrence and adjuvant chemotherapy benefit in patients with early-stage colon cancer. J. Cell. Mol. Med. 24, 3229–3241.

13. Lin, L., Que, Y., Lu, P., Li, H., Xiao, M., Zhu, X., and Li, D. (2020). Chidamide inhibits acute myeloid leukemia cell proliferation by lncRNA VPS9D1-AS1 downregulation via MEK/ERK signaling pathway. Front. Pharmacol. 11, 569651.

14. Peng, W., Zhang, C., Peng, J., Huang, Y., Peng, C., Tan, Y., Ji, D., Zhang, Y., Zhang, D., Tang, J., et al. (2020). lnc-FAM84B-4 acts as an oncogenic lncRNA by interacting with protein hnRNPK to restrain MAPK phosphatases-DUSP1 expression. Cancer Lett. 494, 94–106.

15. Li, Y., Yin, Z.R., Fan, J.S., Zhang, S.Y., and Yang, W.B. (2019). The roles of exosomal miRNAs and lncRNAs in lung diseases. Signal Transduct. Target. Ther. 4, 47.

16. Mu, Y., Tang, Q., Feng, H., Zhu, L., and Wang, Y. (2020). lncRNA KTN1-AS1 promotes glioma cell proliferation and invasion by negatively regulating miR-505-3p. Oncol. Rep. 44, 2645–2655.

17. Aleksakhina, S.N., Kashyap, A., and Imyanitov, E.N. (2019). Mechanisms of acquired tumor drug resistance. Biochim. Biophys. Acta Rev. Cancer 1872, 188310.

18. Zhang, P.F., Pei, X., Li, K.S., Jin, L.N., Wang, F., Wu, J., and Zhang, X.M. (2019). Circular RNA circFGFR1 promotes progression and anti-PD-1 resistance by sponging miR-381-3p in non-small cell lung cancer cells. Mol. Cancer 18, 179.

19. Cheng, J., Zhuo, H., Wang, L., Zheng, W., Chen, X., Hou, J., Zhao, J., and Cai, J. (2020). Identification of the combinatorial effect of miRNA family regulatory network in different growth patterns of GC. Mol. Ther. Oncolytics 17, 531–546.

20. Bao, W.D., Zhou, X.T., Zhou, L.T., Wang, F., Yin, X., Lu, Y., Zhu, L.Q., and Liu, D. (2020). Targeting miR-124/Ferroportin signaling ameliorated neuronal cell death through inhibiting apoptosis and ferroptosis in aged intracerebral hemorrhage murine model. Aging Cell 19, e13235.

21. Tian, X., Yu, H., Li, D., Jin, G.J., Dai, S.D., Gong, P.C., Kong, C.C., and Wang, X.J. (2020). The miR-5694/AF9/Snail axis provides metastatic advantages and a therapeutic target in basal-like breast cancer. Mol. Ther. Published online November 20, 2020. https://doi.org/10.1016/j.ymthe.2020.11.022.

22. Salmena, L., Poliseno, L., Tay, Y., Kats, L., and Pandolfi, P.P. (2011). A ceRNA hypothesis: the Rosetta Stone of a hidden RNA language? Cell 146, 353–358.

23. Zhan, M., He, K., Xiao, J., Liu, F., Wang, H., Xia, Z., Duan, X., Huang, R., Li, Y., He, X., et al. (2018). lncRNA HOXA11-AS promotes hepatocellular carcinoma progression by repressing miR-214-3p. J. Cell. Mol. Med. 22, 3758–3767.

24. Zhang, Y., Huang, C., Zhu, Z., Hou, Y., Huang, S., Sun, C., Tang, Y., Zhang, Z., Wang, L., Chen, H., et al. (2020). lncRNA NEAT1 regulates the proliferation and migration of hepatocellular carcinoma cells by acting as a miR-320a molecular sponge and targeting L antigen family member 3. Int. J. Oncol. 57, 1001–1012.

25. Xu, D., Liu, X., Wu, J., Wang, Y., Zhou, K., Chen, W., Chen, J., Chen, C., and Chen, L. (2020). lncRNA WWOX-AS1 sponges miR-20b-5p in hepatocellular carcinoma and represses its progression by upregulating WWOX. Cancer Biol. Ther. 21, 927–936.

26. Zhao, C., Tao, T., Yang, L., Qin, Q., Wang, Y., Liu, H., Song, R., Yang, X., Wang, Q., Gu, S., et al. (2019). Loss of PDZK1 expression activates PI3K/AKT signaling via PTEN phosphorylation in gastric cancer. Cancer Lett. 453, 107–121.

27. Cao, L.Q., Yang, X.W., Chen, Y.B., Zhang, D.W., Jiang, X.F., and Xue, P. (2019). Exosomal miR-21 regulates the TETs/PTENp1/PTEN pathway to promote hepatocellular carcinoma growth. Mol. Cancer 18, 148.

28. Zhen, L., Zhao, Q., Lü, J., Deng, S., Xu, Z., Zhang, L., Zhang, Y., Fan, H., Chen, X., Liu, Z., et al. (2020). miR-301a-PTEN-AKT signaling induces cardiomyocyte proliferation and promotes cardiac repair post-MI. Mol. Ther. Nucleic Acids 22, 251–262.

29. Zhang, X., Wang, D., Liu, B., Jin, X., Wang, X., Pan, J., Tu, W., and Shao, Y. (2020). IMP3 accelerates the progression of prostate cancer through inhibiting PTEN expression in a SMURF1-dependent way. J. Exp. Clin. Cancer Res. 39, 190.

30. Sun, L.L., Xiao, L., Du, X.L., Hong, L., Li, C.L., Jiao, J., Li, W.D., and Li, X.Q. (2019). miR-205 promotes endothelial progenitor cell angiogenesis and deep vein thrombosis recanalization and resolution by targeting PTEN to regulate Akt/autophagy pathway and MMP2 expression. J. Cell. Mol. Med. 23, 8493–8504.

31. Wu, W., Jing, D., Meng, Z., Hu, B., Zhong, B., Deng, X., Jin, X., and Shao, Z. (2020). FGD1 promotes tumor progression and regulates tumor immune response in osteosarcoma via inhibiting PTEN activity. Theranostics 10, 2859–2871.

32. Yu, F., Chen, B., Dong, P., and Zheng, J. (2020). HOTAIR epigenetically modulates PTEN expression via microRNA-29b: a novel mechanism in regulation of liver fibrosis. Mol. Ther. 28, 2703.

33. Mu, M., Niu, W., Zhang, X., Hu, S., and Niu, C. (2020). lncRNA BCYRN1 inhibits glioma tumorigenesis by competitively binding with miR-619-5p to regulate CUEDC2 expression and the PTEN/AKT/p21 pathway. Oncogene 39, 6879–6892.

34. Tseng, L.L., Cheng, H.H., Yeh, T.S., Huang, S.C., Syu, Y.Y., Chuu, C.P., Yuh, C.H., Kung, H.J., and Wang, W.C. (2020). Targeting the histone demethylase PHF8-mediated PKCα-Src-PTEN axis in HER2-negative gastric cancer. Proc. Natl. Acad. Sci. USA 117, 24859–24866.

35. Hutchings, C., Phillips, J.A., and Djamgoz, M.B.A. (2020). Nerve input to tumours: pathophysiological consequences of a dynamic relationship. Biochim. Biophys. Acta Rev. Cancer 1874, 188411.

36. Cai, L., Ye, Y., Jiang, Q., Chen, Y., Lyu, X., Li, J., Wang, S., Liu, T., Cai, H., Yao, K., et al. (2015). Epstein-Barr virus-encoded microRNA BART1 induces tumour metastasis by regulating PTEN-dependent pathways in nasopharyngeal carcinoma. Nat. Commun. 6, 7353.

37. Azimi, F., Scolyer, R.A., Rumcheva, P., Moncrieff, M., Murali, R., McCarthy, S.W., Saw, R.P., and Thompson, J.F. (2012). Tumor-infiltrating lymphocyte grade is an independent predictor of sentinel lymph node status and survival in patients with cutaneous melanoma. J. Clin. Oncol. 30, 2678–2683.

38. Siemers, N.O., Holloway, J.L., Chang, H., Chasalow, S.D., Ross-MacDonald, P.B., Voliva, C.F., and Szustakowski, J.D. (2017). Genome-wide association analysis identifies genetic correlates of immune infiltrates in solid tumors. PLoS ONE 12, e0179726.

39. Hu, J., Dong, Y., Ding, L., Dong, Y., Wu, Z., Wang, W., Shen, M., and Duan, Y. (2019). Local delivery of arsenic trioxide nanoparticles for hepatocellular carcinoma treatment. Signal Transduct. Target. Ther. 4, 28.

40. Ma, Y.S., Chu, K.J., Ling, C.C., Wu, T.M., Zhu, X.C., Liu, J.B., Yu, F., Li, Z.Z., Wang, J.H., Gao, Q.X., et al. (2020). Long noncoding RNA OIP5-AS1 promotes the progression of liver hepatocellular carcinoma via regulating the hsa-miR-26a-3p/EPHA2 axis. Mol. Ther. Nucleic Acids 21, 229–241.

41. Zhao, Y., Zhang, Y.N., Wang, K.T., and Chen, L. (2020). Lenvatinib for hepatocellular carcinoma: from preclinical mechanisms to anti-cancer therapy. Biochim. Biophys. Acta Rev. Cancer 1874, 188391.

42. Jasirwan, C.O.M., Hasan, I., Sulaiman, A.S., Lesmana, C.R.A., Kurniawan, J., Kalista, K.F., Nababan, S.H., and Gani, R.A. (2020). Risk factors of mortality in the patients with hepatocellular carcinoma: a multicenter study in Indonesia. Curr. Probl. Cancer 44, 100480.

43. Wang, Z., Yu, W., Qiang, Y., Xu, L., Ma, F., Ding, P., Shi, L., Chang, W., Mei, Y., and Ma, X. (2020). LukS-PV inhibits hepatocellular carcinoma progression by downregulating HDAC2 expression. Mol. Ther. Oncolytics 17, 547–561.

44. Wei, L., Wang, X., Lv, L., Liu, J., Xing, H., Song, Y., Xie, M., Lei, T., Zhang, N., and Yang, M. (2019). The emerging role of microRNAs and long noncoding RNAs in drug resistance of hepatocellular carcinoma. Mol. Cancer 18, 147.

45. Li, Y., Li, G., Tao, T., Kang, X., Liu, C., Zhang, X., Wang, C., Li, C., and Guo, X. (2019). The μ-opioid receptor (MOR) promotes tumor initiation in hepatocellular carcinoma. Cancer Lett. 453, 1–9.

46. Kim, Y., Jo, M., Schmidt, J., Luo, X., Prakash, T.P., Zhou, T., Klein, S., Xiao, X., Post, N., Yin, Z., and MacLeod, A.R. (2019). Enhanced potency of GalNAc-conjugated antisense oligonucleotides in hepatocellular cancer models. Mol. Ther. 27, 1547–1557.

47. Gong, Z., Yu, J., Yang, S., Lai, P.B.S., and Chen, G.G. (2020). FOX transcription factor family in hepatocellular carcinoma. Biochim. Biophys. Acta Rev. Cancer 1874, 188376.

48. Yuan, F., Zhang, Y., Ma, L., Cheng, Q., Li, G., and Tong, T. (2017). Enhanced NOLC1 promotes cell senescence and represses hepatocellular carcinoma cell proliferation by disturbing the organization of nucleolus. Aging Cell 16, 726–737.

49. Zhang, Q., Song, G., Yao, L., Liu, Y., Liu, M., Li, S., and Tang, H. (2018). miR-3928v is induced by HBx via NF-κB/EGR1 and contributes to hepatocellular carcinoma malignancy by down-regulating VDAC3. J. Exp. Clin. Cancer Res. 37, 14.

50. Ping, Y., Zhou, Y., Hu, J., Pang, L., Xu, C., and Xiao, Y. (2020). Dissecting the functional mechanisms of somatic copy-number alterations based on dysregulated ceRNA networks across cancers. Mol. Ther. Nucleic Acids 21, 464–479.

51. Yang, X.Z., Cheng, T.T., He, Q.J., Lei, Z.Y., Chi, J., Tang, Z., Liao, Q.X., Zhang, H., Zeng, L.S., and Cui, S.Z. (2018). LINC01133 as ceRNA inhibits gastric cancer progression by sponging miR-106a-3p to regulate APC expression and the Wnt/β-catenin pathway. Mol. Cancer 17, 126.

52. Han, Q., Li, J., Xiong, J., and Song, Z. (2020). Long noncoding RNA LINC00514 accelerates pancreatic cancer progression by acting as a ceRNA of miR-28-5p to upregulate Rap1b expression. J. Exp. Clin. Cancer Res. 39, 151.

53. Man, X., Piao, C., Lin, X., Kong, C., Cui, X., and Jiang, Y. (2019). USP13 functions as a tumor suppressor by blocking the NF-kB-mediated PTEN downregulation in human bladder cancer. J. Exp. Clin. Cancer Res. 38, 259.

54. Liu, J., Ding, J., Qu, B., Liu, J., Song, X., Suo, Q., Zhou, A., and Yang, J. (2020). circPSMC3 alleviates the symptoms of PCOS by sponging miR-296-3p and regulating PTEN expression. J. Cell. Mol. Med. 24, 11001–11011.

55. Yang, B., Feng, X., Liu, H., Tong, R., Wu, J., Li, C., Yu, H., Chen, Y., Cheng, Q., Chen, J., et al. (2020). High-metastatic cancer cells derived exosomal miR92a-3p promotes epithelial-mesenchymal transition and metastasis of low-metastatic cancer cells by regulating PTEN/Akt pathway in hepatocellular carcinoma. Oncogene 39, 6529–6543.

56. Stroese, A.J., Ullerich, H., Koehler, G., Raetzel, V., Senninger, N., and Dhayat, S.A. (2018). Circulating microRNA-99 family as liquid biopsy marker in pancreatic adenocarcinoma. J. Cancer Res. Clin. Oncol. 144, 2377–2390.

57. Dhayat, S.A., Mardin, W.A., Seggewiß, J., Ströse, A.J., Matuszcak, C., Hummel, R., Senninger, N., Mees, S.T., and Haier, J. (2015). MicroRNA profiling implies new markers of gemcitabine chemoresistance in mutant p53 pancreatic ductal adenocarcinoma. PLoS ONE 10, e0143755.

58. Sun, G., Li, Z., He, Z., Wang, W., Wang, S., Zhang, X., Cao, J., Xu, P., Wang, H., Huang, X., et al. (2020). Circular RNA MCTP2 inhibits cisplatin resistance in gastric cancer by miR-99a-5p-mediated induction of MTMR3 expression. J. Exp. Clin. Cancer Res. 39, 246.

59. Zhang, H., Chen, X., and Yuan, Y. (2020). Investigation of the miRNA and mRNA coexpression network and their prognostic value in hepatocellular carcinoma. BioMed Res. Int. 2020, 8726567.

60. Song, S.K., Jung, W.Y., Park, S.K., Chung, C.W., and Park, Y. (2019). Significantly different expression levels of microRNAs associated with vascular invasion in hepatocellular carcinoma and their prognostic significance after surgical resection. PLoS ONE 14, e0216847.

61. Sun, X., Liu, X., Wang, Y., Yang, S., Chen, Y., and Yuan, T. (2018). miR-100 inhibits the migration and invasion of nasopharyngeal carcinoma by targeting IGF1R. Oncol. Lett. 15, 8333–8338.

62. Agosto-Arroyo, E., Isayeva, T., Wei, S., Almeida, J.S., and Harada, S. (2017). Differential gene expression in ductal carcinoma in situ of the breast based on ERBB2 status. Cancer Contr. 24, 102–110.

63. Thean, L.F., Wong, Y.H., Lo, M., Loi, C., Chew, M.H., Tang, C.L., and Cheah, P.Y. (2017). Chromosome 19q13 disruption alters expressions of CYP2A7, MIA and MIA-RAB4B lncRNA and contributes to FAP-like phenotype in APC mutation-negative familial colorectal cancer patients. PLoS ONE 12, e0173772.

64. Chen, Y., Ren, B., Yang, J., Wang, H., Yang, G., Xu, R., You, L., and Zhao, Y. (2020). The role of histone methylation in the development of digestive cancers: a potential direction for cancer management. Signal Transduct. Target. Ther. 5, 143.

65. Khalaj-Kondori, M., Hosseinnejad, M., Hosseinzadeh, A., Behroz Sharif, S., and Hashemzadeh, S. (2020). Aberrant hypermethylation of OGDHL gene promoter in sporadic colorectal cancer. Curr. Probl. Cancer 44, 100471.

66. Yan, J.B., Lai, C.C., Jhu, J.W., Gongol, B., Marin, T.L., Lin, S.C., Chiu, H.Y., Yen, C.J., Wang, L.Y., and Peng, I.C. (2020). Insulin and metformin control cell proliferation by regulating TDG-mediated DNA demethylation in liver and breast cancer cells. Mol. Ther. Oncolytics 18, 282–294.

67. Shu, W.J., and Du, H.N. (2020). The methyltransferase SETD3-mediated histidine methylation: biological functions and potential implications in cancers. Biochim. Biophys. Acta Rev. Cancer 1875, 188465.

68. Jin, Y., Chen, D.L., Wang, F., Yang, C.P., Chen, X.X., You, J.Q., Huang, J.S., Shao, Y., Zhu, D.Q., Ouyang, Y.M., et al. (2020). The predicting role of circulating tumor DNA landscape in gastric cancer patients treated with immune checkpoint inhibitors. Mol. Cancer 19, 154.

69. Yang, C.Y., Fan, M.H., Miao, C.H., Liao, Y.J., Yuan, R.H., and Liu, C.L. (2020). Engineering chimeric antigen receptor T cells against immune checkpoint inhibitors PD-1/PD-L1 for treating pancreatic cancer. Mol. Ther. Oncolytics 17, 571–585.

70. Zhang, L.M., Wang, W., Wang, R.K., Zhang, N.C., Shang, H., Bi, Y., Chen, D., Zhang, C.Z., Li, L., Yin, J., et al. (2020). Reshaping the immune microenvironment by oncolytic herpes simplex virus in murine pancreatic ductal adenocarcinoma. Mol. Ther. Published online October 30, 2020. https://doi.org/10.1016/j.ymthe.2020.10.027.

71. van den Ende, T., van den Boorn, H.G., Hoonhout, N.M., van Etten-Jamaludin, F.S., Meijer, S.L., Derks, S., de Gruijl, T.D., Bijlsma, M.F., van Oijen, M.G.H., and van Laarhoven, H.W.M. (2020). Priming the tumor immune microenvironment with chemo(radio)therapy: a systematic review across tumor types. Biochim. Biophys. Acta Rev. Cancer 1874, 188386.

72. He, J.W., Zhou, X.J., Lv, J.C., and Zhang, H. (2020). Perspectives on how mucosal immune responses, infections and gut microbiome shape IgA nephropathy and future therapies. Theranostics 10, 11462–11478.

73. Yamada, K., and Herzog, R.W. (2020). When immune suppression goes wrong. Mol. Ther. 28, 1381–1382.

74. Zhu, M., Deng, G., Tan, P., Xing, C., Guan, C., Jiang, C., Zhang, Y., Ning, B., Li, C., Yin, B., et al. (2020). Beclin 2 negatively regulates innate immune signaling and tumor development. J. Clin. Invest. 130, 5349–5369.

75. Hamarsheh, S., Groß, O., Brummer, T., and Zeiser, R. (2020). Immune modulatory effects of oncogenic KRAS in cancer. Nat. Commun. 11, 5439.